AN IMPROVED HATCH FILTER WITH ADAPTIVE SMOOTHING WINDOW WIDTH FOR BDS SINGLE-FREQUENCY POSITIONING

Yi JIANG[1], Han SHAO[2*], Yue FAN[3]

An improved Hatch filter proposed in this paper can adaptively adjust its smoothing window width according to Carrier-to-Noise Ratio (CNR). We collected actual BeiDou Navigation Satellite System (BDS) data for the experimental verification and utilizes BDS Klobuchar model to correct the ionospheric model. The experimental results show that, compared with the traditional Hatch filter, errors of the improved algorithm in the range domain and the position domain are reduced by 28% and 17%, respectively. Considering the extensive development of BDS single-frequency positioning, this proposed algorithm is of great value both in theory and practice.

Keywords: GNSS, BeiDou Navigation Satellite System (BDS), Hatch filter, Smoothing window width, Ionospheric delay, Klobuchar model

1. Introduction

In November 2019, several standardized documents for high precision applications of BeiDou Satellite Navigation System (BDS) were published by China with the launch of the 51-th BDS satellite. It means that the receiver users are now able to obtain the definition and description of the detailed parameters directly, rather than relying on other Global Navigation Satellite System (GNSS). The BDS receiver can obtain data in two forms: pseudorange observation and carrier phase observation [1]. The pseudorange observation is the pseudo-distance between the satellite and the user, as it contains various errors, such as the clock correction and the atmospheric delay. Currently, its measurement error can even reach tens of meters in the BDS receivers [2]. In contrast, as a cumulative observation result, the measurement error of the carrier phase can be controlled between 1 m and 5 m, but the fix ambiguity problem persists. There are significant differences between the two, but they can be complementary in the positioning process [3].

[1] A.P., Information Science and Technology College, Dalian Maritime University, China, E-mail: j_y@dlmu.edu.cn

[2*] Graduate student, Information Science and Technology College, Dalian Maritime University, China, E-mail: shaohan@dlmu.edu.cn

[3] Graduate student, Information Science and Technology College, Dalian Maritime University, China, E-mail: F_Yuee@163.com

To improve the positioning precision, common algorithm is based on a Hatch filter, which combines the pseudorange observation and the carrier phase observation into an accurate measurement [4]. Traditional Hatch filter is formulated in a simple Kalman filter based structure to give more flexibility and better performance [5]. Moreover, due to its simple structure and fast calculation, Hatch filter plays an important role in pseudorange smoothing, especially in single-frequency GNSS receivers with low cost.

A smoothing window width is designed to determine the weight of the two observations in the traditional Hatch filter. Generally, the value of the smoothing window width is invariant based on human experience or another auxiliary system [6]. The larger the value is, the better the smoothing performance will be. However, if the value of the smoothing window width is too large, other problems will appear, such as the ionospheric divergence. On the contrary, it may aggravate the multipath effect if the value is too small [7]. Hence, the smoothing window width should vary according to the distinct regions, environments and signal intensity [8]. In the traditional Hatch filter, the value of the smoothing window width is generally between 50 and 200 [9]. However, due to the lack of theoretical basis, using this subjective setting method is difficult to achieve the desired smoothing effect.

Hitherto, several strategies for the calculation of the smoothing window width have been proposed. Zhou suggested using Doppler smoothing codes to adjust the smoothing window width [10]. Jang analyzed the divergence-free characteristics of dual-frequency Satellite-Based Augmentation System (SBAS) to give the smoothing window width [11]. Zhao presented a method to make the smoothing window width vary with the ionospheric delay and the multipath effect with Local Area Augmentation System (LAAS) [12]. However, most of the proposed algorithms are based on SBAS and LAAS for ionospheric correction, and there are few studies on the smoothing window width for GNSS single-frequency receiver without an auxiliary system. To increase the accuracy of the low-cost single-frequency receiver, an improved Hatch filter proposed here can adaptively regulate its smoothing window width according to Carrier-to-Noise Ratio (CNR). Compared with the previous studies, the proposed algorithm computes the smoothing window width with a single-frequency BDS receiver, rather than relying on the information of differential GNSS. Based on the Hatch filter structure, the advantages of the simple and easy implementation for the single-frequency positioning is preserved. Moreover, the proposed algorithm alleviates the problem of ionospheric divergence using the variable smoothing window width and reduces the positioning error consequently.

The remainder of the paper is organized as follows. The traditional Hatch filter will be reviewed in Section 2. Section 3 presents the improved Hatch Filter and gives the analytical expression of the adaptive smoothing window width

according to the Mean Square Error (MSE) criterion. Section 4 describes the proposed algorithm implementation, which verifies the feasibility of the improved Hatch filter in theory. Performance analysis in range domain and discussion of positioning error under static positioning using actual BDS data are given in Section 5. Lastly, the conclusion is drawn in Section 6.

2. Traditional Hatch Filter

BDS pseudorange observation equation at the *k*th epoch can be described as [3]

$$\rho_k = r_k + c\delta t_k + I_k + T_k + \varepsilon_{\rho,k} \tag{1}$$

where δt_k denotes the clock biases; ρ_k and r_k are the pseudorange observation and the true geometric range between the satellite and the receiver, respectively; I_k and T_k are the ionospheric delay and the tropospheric delay, respectively; $\varepsilon_{\rho,k}$ represents the measurement error of the pseudorange observation.

Likewise, the carrier phase observation equation at the *k*th epoch is defined as [3]

$$\lambda\phi_k = r_k + c\delta t_k - I_k + T_k + \lambda N + \varepsilon_{\varphi,k} \tag{2}$$

where ϕ_k and λ are correspondingly the carrier phase and the carrier wavelength; N is the integer ambiguity; $\varepsilon_{\varphi,k}$ represents the measurement error of the carrier phase.

It is assumed that the receiver is in a carrier locked state, i.e. the integer ambiguity always remains constant. Thus, the observations of two adjacent epochs can be subtracted to get

$$\Delta\rho_k = \Delta r_k + c\Delta\delta t_k + \Delta I_k + \Delta T_k + \Delta\varepsilon_{\rho,k} \tag{3}$$

$$\lambda \cdot \Delta\phi_k = \Delta r_k + c\Delta\delta t_k - \Delta I_k + \Delta T_k + \Delta\varepsilon_{\varphi,k} \tag{4}$$

Ideally, $\Delta\phi_k$ is the integral Doppler from the (*k*-1)th to the *k*th epoch, whose accuracy can reach centimeter level. Now, substituting the equation (4) into equation (3) such that the variation of the pseudorange observation $\Delta\rho_k$ can be written as

$$\Delta\rho_k = \lambda\Delta\phi_k + 2\Delta I_k + \Delta\varepsilon_{\rho,k} - \Delta\varepsilon_{\varphi,k} \tag{5}$$

If the change of the ionospheric delay ΔI_k is very small, $\Delta\rho_k$ would be approximately equal to the distance $\lambda\Delta\phi_k$. Therefore, equation (5) can be simplified as

$$\Delta\rho_k \approx \lambda\Delta\phi_k \tag{6}$$

Therefore, for two adjacent observations (*k-1*)-th and *k*-th epoch, the recursive equation of carrier phase smoothing pseudorange becomes

$$\hat{\rho}_k = \rho_{k-1} + \lambda\phi_k - \lambda\phi_{k-1} \tag{7}$$

where $\hat{\rho}_k$ is the smoothed pseudorange.

After several iterations, the smoothing model of the traditional Hatch filter can be obtained.

$$\hat{\rho}_k = \frac{1}{M}\rho_k + \frac{M-1}{M}[\hat{\rho}_{k-1} + \lambda(\phi_k - \phi_{k-1})] \tag{8}$$

where M denotes the length of the Hatch filter, i.e. smoothing window width.

Based on error propagation theory, it can be deduced from equation (8) that the standard deviation of the smoothed pseudorange error $\sigma_{\hat{\rho}}$ after the Hatch filter.

$$\sigma_{\hat{\rho}}^2 = \frac{1}{M}\sigma_\rho^2 + \frac{M+1}{M}\sigma_\phi^2 \tag{9}$$

where σ_ρ and σ_ϕ indicate the error standard deviations of the pseudorange observation and the carrier phase observation, respectively.

According to a previous study [13], the precision of the carrier phase observation is much better than that of the pseudorange observation, so that

$$\sigma_{\hat{\rho}} \approx \frac{1}{\sqrt{M}}\sigma_\rho \tag{10}$$

As indicated by equation (10), Hatch filter has a compression effect on the error of the pseudorange observation without considering the ionospheric delay error variation, which leads to a more accurate pseudorange than that without smoothing. Moreover, it is superior in single-frequency positioning by canceling out the integer ambiguity.

3. Adaptive Hatch Filter

The traditional Hatch filter has a significant defect according to equation (8). If the initial value of the smoothed pseudorange has a large deviation, the smoothing method needs to run for a very long time to gradually eliminate the deviation. Therefore, for the traditional Hatch filter, the initial value of smoothed pseudorange should be as precise as possible. To get a more accurate initial value $\hat{\rho}_1$, it should be estimated for a while firstly, and the average is calculated as $\hat{\rho}_1$.

$$\hat{\rho}_1 = \frac{1}{M}\sum_{i=k-M+1}^{k}[\rho_i - \lambda(\phi_i - \phi_1)] \tag{11}$$

Assuming that an accurate initial value $\hat{\rho}_1$ can be obtained, the carrier phase variation can be completely supplanted by the variation of the pseudorange observation as an effective integration method.

$$\hat{\rho}_k = \hat{\rho}_1 + \lambda\left(\phi_k - \phi_1\right) \tag{12}$$

Then, substituting equation (11) into equation (12), so that the traditional Hatch filter can be reformulated as

$$\hat{\rho}_k = \frac{1}{M}\sum_{i=k-M+1}^{k}(\rho_i - \lambda\phi_i) + \lambda\phi_k \tag{13}$$

From equation (6), the ionospheric delay is ignored in the traditional Hatch filter. However, even when the ionospheric delay varies slowly, a considerable ionospheric divergence error accumulates gradually as the smoothing epoch increases [14].

Considering the ionospheric delay, the measurement error of the two observations, the smoothed pseudorange $\hat{\rho}_k$ may be expressed as

$$\hat{\rho}_k = \rho_T - \frac{2}{M}\sum_{i=k-M+1}^{k} I_i + 2I_k + \frac{1}{M}\sum_{i=k-M+1}^{k}\varepsilon_{\rho,i} - \frac{1}{M}\sum_{i=k-M+1}^{k}\varepsilon_{\varphi,i} + \varepsilon_{\varphi,k} \tag{14}$$

where ρ_T is the distance from the satellite to the receiver considering the ionospheric delay error at the kth epoch.

As noted earlier, the smoothing window width M is a key parameter affecting the performance of the Hatch filter. Generally, its value is invariant based on human experience or augmentation another auxiliary system, which may aggravate the ionospheric divergence [15]. Hence it is essential to determine the smoothing window width M, especially in the BDS single-frequency positioning.

From equation (14), the smoothed pseudorange $\hat{\rho}_k$ can be divided into two components, namely pseudorange ρ_T with the ionospheric delay error at the kth epoch and other error $\delta\rho_k$. It can be expressed as

$$\begin{aligned}\hat{\rho}_k &= \rho T + \delta\rho_k \\ &= \rho T + N_k + R_k\end{aligned} \tag{15}$$

where N_k and R_k represent the cumulative error of the pseudorange observation and the ionospheric delay at the kth epoch, respectively.

The cumulative error of the pseudorange observation N_k is due to the DLL tracking error, which includes the thermal errors of the receiver and the multipath effect. Since the measurement precision of the carrier phase observation is better than that of the pseudorange observation, it can be derived as

$$\begin{aligned} N_k &= \frac{1}{M}\sum_{\mathrm{i}=k-M+1}^{k}\varepsilon_{\rho,i} - \frac{1}{M}\sum_{i=k-M+1}^{k}\varepsilon_{\varphi,i} + \varepsilon_{\varphi,k} \\ &\approx \frac{1}{M}\sum_{i=k-M+1}^{k}\varepsilon_{\rho,i} \end{aligned} \tag{16}$$

then

$$\begin{aligned} E(N_k^T N_k) &= \frac{(\varepsilon_{\rho,k} + \cdots + \varepsilon_{\rho,k-M+1})^T (\varepsilon_{\rho,k} + \cdots + \varepsilon_{\rho,k-M+1})}{M^2} \\ &= \frac{1}{M^2}\{\sigma_{\rho,k}^2 + \sigma_{\rho,k\text{-}1}^2 + \cdots + \sigma_{\rho,k\text{-}M+1}^2\} \approx \frac{1}{M}\bar{\sigma}^2 \end{aligned} \tag{17}$$

where $\bar{\sigma}^2$ denotes the Code Measurement Error (CME).

Likewise,

$$\begin{aligned} R_k &= -\frac{2}{M}\sum_{i=k-M+1}^{k} I_i + 2I_k \\ &= \frac{2}{M}\sum_{i=k-M+1}^{k}(I_k - I_i) = (M-1)\bar{I} \end{aligned} \tag{18}$$

where $\bar{I}$ is the average time variation rate of the ionospheric delay, which varies slowly with time and can be decomposed into a constant deviation I_0 and a slope deviation I_d [16].

$$I(t) = I_0 + I_d t \tag{19}$$

when the sun keeps a middle-low active state, the slope deviation I_d in the mid-latitude region usually obeys normal distribution, and the magnitude ordinarily less than 0.1 m/min [17].

Generally, I_d is calculated by the BDS Klobuchar model with 8 parameters [18]. This model utilizes the variables such as the geographic longitude of the ionosphere pierce point to estimate the ionospheric delay, which is suitable for the mid-latitude region and has already widely used in BDA receivers nowadays.

$$I_d = 5\times10^{-9} + A\cos\frac{2\pi}{T}(t - 50400) \tag{20}$$

where A and T represent the amplitude and period of the cosine function respectively, which can be calculated from the parameters of BDS Navigation Ephemeris File.

From (15), Mean Square Error (MSE) after the Hatch filter is

$$\begin{aligned} \mathrm{MSE} &= E[\delta\rho_k^T \delta\rho_k] \\ &= E[(N_k + R_k)^T (N_k + R_k)] \end{aligned} \tag{21}$$

Substitute equations (18) and (19) into equation (21),

$$\mathrm{MSE} = \frac{1}{M}\bar{\sigma}^2 + (M-1)^2 \bar{I}^2 \tag{22}$$

According to equation (22), we can see that the magnitude of the MSE is related to the smoothing window width *M*. As a result, the optimal *M* should satisfy (23) to minimize MSE.

$$\frac{d}{dM}\mathrm{MSE} = 2(M-1)\bar{I}^2 - \frac{1}{M^2}\bar{\sigma}^2 = 0 \tag{23}$$

We know that equation （23） has a real root and two conjugate virtual roots according to Cardano formula [19]. Here only real roots need to be solved, so the optimal *M* is

$$M_{\mathrm{temp}} = \sqrt[3]{\frac{1}{2}(-q + \sqrt{q^2 + 4p^3})} + \sqrt[3]{\frac{1}{2}(-q - \sqrt{q^2 + 4p^3})} + \frac{1}{3} \tag{24}$$

Where $p = \frac{1}{3}(-\frac{1}{3}), q = -\frac{2}{27} - \frac{\bar{\sigma}^2}{2\bar{I}^2}$

Since the incoherent DLL discriminator is used for tracking, $\bar{\sigma}^2$ calculated by the thermal noise distance error flutter formula [20] can be expressed as

$$\bar{\sigma} = \frac{180^\circ}{\pi}\sqrt{\frac{B}{\mathrm{C/N_0}}\left(1 + \frac{1}{2T\mathrm{C/N_0}}\right)} \tag{25}$$

where C/No is the CNR of satellite signals, *B* denotes the noise bandwidth, *T* represents the integration time.

Finally, as the smoothing window width *M* is an integer, we need to round it up during the calculation.

$$M = \mathrm{round}\ （M_{\mathrm{temp}}） \tag{26}$$

Compared with previous studies, the adaptive Hatch filter proposed here considers both the CME and the ionospheric delay. As the key parameter, the smoothing window width can vary depending on CNR. Furthermore, it also solves the drawbacks of previous empirical setting without any auxiliary system.

4. Algorithm Implementation

Before exploiting the above algorithm in the actual scenario, it is necessary to carry out the algorithm implementation and theoretical verification. Fig. 1 schematically displays a structure block diagram of BDS single-frequency

positioning based on the adaptive Hatch filter. As input components of the adaptive Hatch filter, BDS Klobuchar model and DLL discriminator are correspondingly determined by equations (20) and (25). Then, without any aid of the auxiliary system, the improved Hatch filter adjusts the smoothing window width based on the current CNR. Finally, Position, Velocity and Time (PVT) solution is solved.

As noted earlier, unlike the traditional Hatch filter, the improved algorithm not only optimizes the initial value, but also can apply the optimal smoothing window according to the satellite status of each channel. Fig. 2 shows the block diagram comparison of the traditional Hatch filter and the proposed adaptive Hatch filter. The initial value average is derived by equation (13) with the pseudorange observations and the carrier phase observations. At the same time, the optimal M is calculated separately at each epoch by equation (24) for the smoothing processing. Eight satellite channels are applied in this paper.

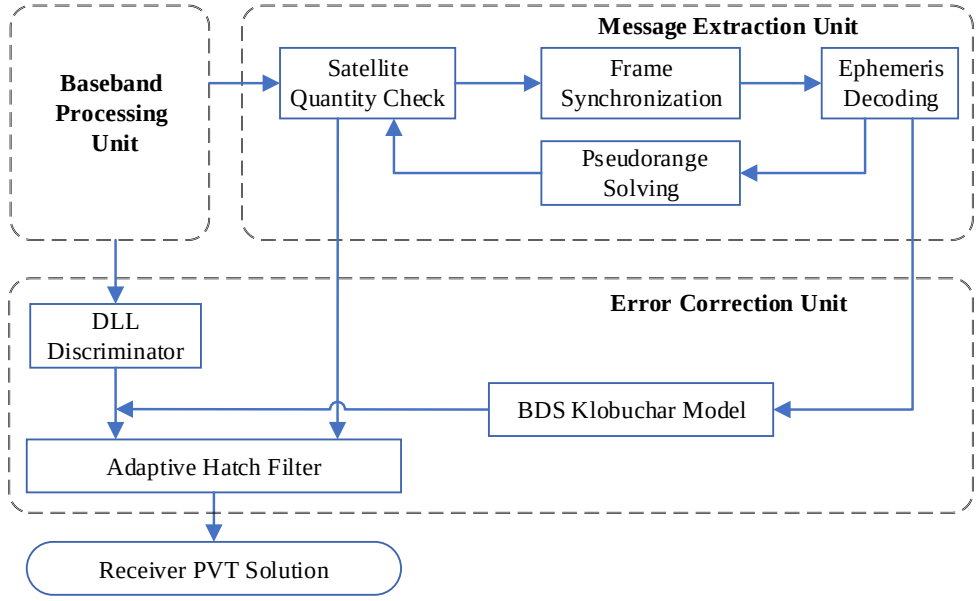

Fig. 1. Block Diagram of BDS Single-frequency Positioning Based on Adaptive Hatch Filter

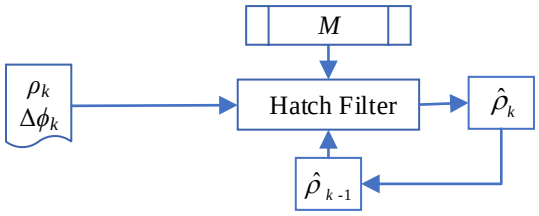

(a) Traditional Hatch Filter

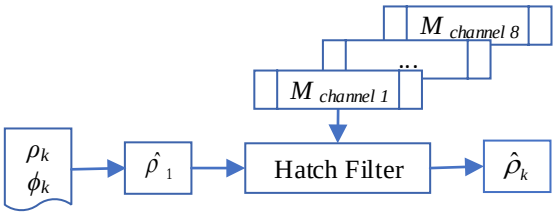

(b) Adaptive Hatch Filter

Fig. 2. Process of Traditional Hatch Filter and Adaptive Hatch Filter

In this instance, from equation (22), MSE can be indicated as Fig. 3. The arrow in Fig. 3 points to the normal direction of the current data node, that is, the variation direction of MSE.

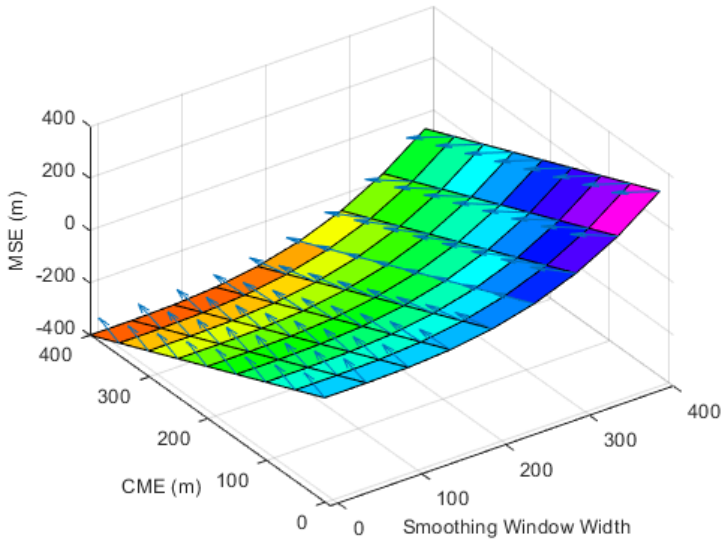

Fig. 3. MSE after Hatch Filter

Obviously, the ideal *M* should be limited to between 50 and 200, which is coincident with the range in the traditional Hatch filter based on human experience. However, when *M* is greater than 200, the MSE of pseudorange observation increases rapidly, and the normal direction almost coincides with the horizontal direction. Therefore, if the value of *M* is irrational (i.e. greater than 200), the positioning accuracy using the Hatch filter would be worse on the contrary. This phenomenon is verified in the subsequent real experiments as well.

5. Results and Discussion

5.1. Experimental Scene

To evaluate the performance of the adaptive Hatch filter proposed in this paper, BDS B1 signals are collected by a GNSS HG-SOFTPS04 signal collector of Beidou Xingyuan Navigation Company on a roof of Science Hall in Dalian Maritime University, as shown in Fig. 4. Its exact longitude and latitude coordinates are (121˚31’19.8012’’E, 38˚52’8.5548’’N), and the altitude is 35.580 m. The collected BDS signals are processed by Matlab to verify the availability of the proposed adaptive Hatch filter. The positioning accuracy of the proposed algorithm is compared with that without carrier smoothing and with the traditional Hatch filter.

Fig. 5 displays the Sky Map during the signal collection, in which the blue number represents BDS satellite Pseudo Random Noise code. Seven satellites have been tracked in BDS receiver totally, and the elevation angle of the satellites is between 30 and 210 degrees.

Fig. 4. Satellite Signal Collection Scene

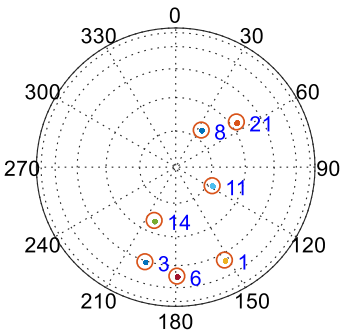

Fig. 5. Sky Map during Signal Collection

5.2. Performance Analysis in Range Domain

The performance of the proposed algorithm is evaluated by the range accuracy and the position accuracy. In the range domain, the error is typically calculated by subtracting the smoothed pseudorange from the true distance value [21], which can evaluate the algorithm performance overall.

To compare the characteristics of the raw algorithm, the traditional Hatch filter and the adaptive Hatch filter, the absolute value of range error is showed in Fig. 6. The raw algorithm refers to the traditional BDS single-frequency receiver without a Hatch filter. In the case of the traditional Hatch filter, 50, 100, 200 and 400 are selected as the smoothing window width.

Fig. 6 shows that, for the current situation, 100 is the suitable smoothing window width for the traditional Hatch filter with a range of 0 to 5m. Compared with the traditional Hatch filter, it is obvious that the jitter amplitude of the adaptive Hatch filter is smaller than the case of M=100. Besides that, we can see that the error with M =400 is the largest, although the jitter amplitude is extremely steady. Its range error keeps about 20m after 500 epochs. The range error without the smoothing process is the most unstable, and the jitter amplitude even appears to reach 20m.

Without an auxiliary system, the improved algorithm reduces the range error due to the smoothing window width that can adjust with the CNR. It should be noted that at the 600th, 1400th and 2700th epoch, a short period jitter occurs simultaneously of the different algorithms. Normally, it is primarily caused by the quality of the satellite signal observations. As indicated in Fig. 6, when M equals 400, the ionospheric error diverges after 500 epochs, which will exceed the compression effect of smoothing processing ultimately. Thus, the inconsequent M will reduce the algorithmic performance on the contrary.

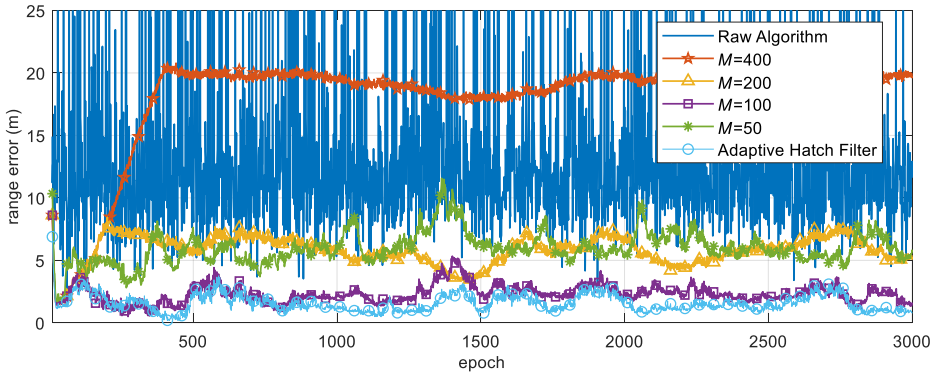

Fig. 6. Range Error under Raw Algorithm, Traditional Hatch Filter (M=50, 100, 200 and 400) and Adaptive Hatch Filter

To compare the smoothing effect, we tabulate the statistics of the range error for all filtering methods shown in Table-1. Six equal-interval periods are selected, each of which contains 500 epochs. The average and maximum errors are also given, respectively.

Table 1

Range error of filtering methods in view

Filtering Method	1	2	3	4	5	6	MAX	AVG
Raw Algorithm	14.8349	14.6194	14.8209	13.8934	14.5539	13.5853	88.481	14.286
M=400	11.7183	19.8440	18.7574	18.9775	19.0532	19.8375	20.782	18.037
M=200	6.0093	6.4759	4.8442	6.0709	5.3647	6.2586	7.923	5.813
M=50	4.3185	4.6154	5.9235	5.0146	5.4520	4.8705	9.754	5.031
M=100	2.2318	2.1835	2.6406	2.6158	2.3273	2.2516	5.334	2.359
Adaptive Hatch Filter	1.9086	1.7391	1.3419	1.9062	1.2633	1.5656	3.637	1.698

Through Table-1, we find that the proposed algorithm outperforms the traditional Hatch filter overall. Compared with the traditional Hatch filter, its average range error and maximum range error are reduced by 28% and 32%, separately, and the positioning accuracy is improved by 19% even at the first interval with the worst performance. Moreover, in the case of the traditional Hatch filter, 100 is suitable for the classical Hatch filter as the typical smoothing window width.

Table-1 also indicates that the range error of the improved algorithm is kept at a minimum level at any time interval, while the filtering effect of the first 500 epoch is not significant in this research. During the first interval, the difference between the range error of the adaptive Hatch filter and the traditional Hatch filter (M=100) is only approximately 0.3 m. However, with the epoch goes, the filtering effect of the proposed algorithm gradually enhances and reaches a stable state. Furthermore, the most severe error occurs in the case where M is 400, even exceeding the range error without Hatch filter. Thus, the necessity of an appropriate setting of M value is demonstrated again.

5.3. Positioning Error Analysis

Like range domain, Root Mean Square Error (RMSE) in position domain is calculated by subtracting the positioning outcome from the truth value of East (E), North (N) and Up (U). The positioning error in three-dimensional space can be obtained as Fig. 7. The precise position (0, 0, 0) of the signal collection scene is marked in yellow. As the earlier analysis in range domain, M is fixed as 100 for Hatch filter in the following discussion to obtain an optimal single-frequency positioning performance. Throughout the session, the positioning error of the improved algorithm is well bound near the yellow mark, which is better than that of the traditional Hatch filter.

Then, RMSE under the raw algorithm, the traditional Hatch filter (M=100) and the adaptive Hatch filter are displayed in Fig. 8 (a), (b) and (c), respectively. Since the amplitude and frequency of the signal jitter decreases by the improved algorithm, the curves in different directions are more concentrated near the zero value. Even at the 1500th epoch with performance degrades, it is obvious that the adaptive Hatch filter demonstrates better positioning accuracy.

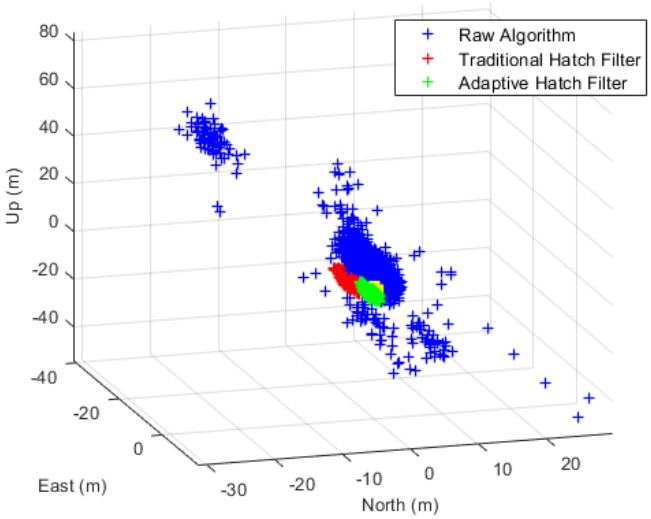

Fig. 7. Positioning Error in Three-dimensional Space under Raw Algorithm, Traditional Hatch Filter (M=100) and Adaptive Hatch Filter

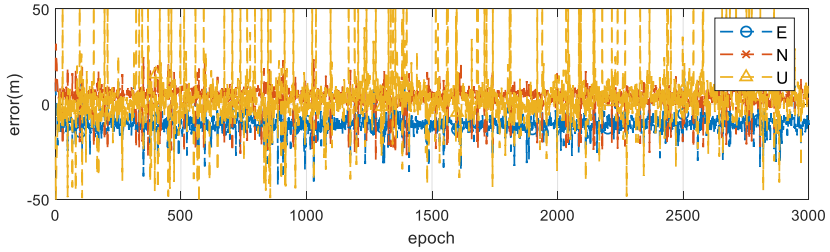

(a) Raw Algorithm

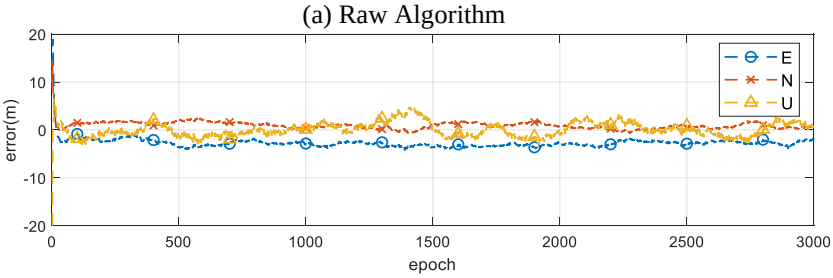

(b) Traditional Hatch Filter (M=100)

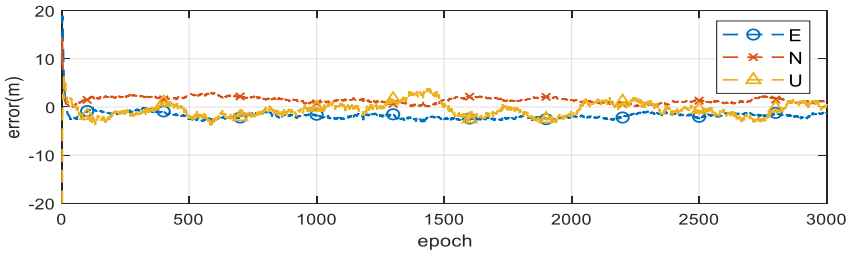

(c) Adaptive Hatch Filter

Fig.8. RMSE in Position Domain

Table 2

RMSE and MSE of positioning errors in three-dimensional under different methods

Filtering Method	E	N	U	Horizontal Error	MSE
Raw Algorithm	11.4405	6.2687	14.6134	8.8546	16.1613
Traditional Hatch Filter (M=100)	1.9128	1.7095	2.3271	1.8112	1.9831
Adaptive Hatch Filter	1.5249	1.5617	1.8533	1.5433	1.6467

Table-2 tabulates the RMSE and MSE of the positioning errors under filtering methods above. As expected, MSE of the presented algorithm applies a reduction of 17% approximately, and RMSE in horizontal and vertical directions are improved by 21% and 15%, respectively. Moreover, compared with the horizontal direction, the positioning of the BDS receiver in the vertical direction is poor in all three cases, but the improved algorithm appears to decrease the RMSE with about 0.5 m. The outcome shows that the adaptive Hatch filter not only theorizes the setting of window smoothing window width, but also improves the positioning accuracy of BDS single-frequency receiver without any auxiliary system.

6. Conclusions

The smoothing window width is one of the key parameters affecting the positioning accuracy of the Hatch filter. Generally, its value is invariant based on human experiences or augmentation system with the lack of theoretical basis. The adaptive Hatch filter proposed here considers both the CME and the ionospheric delay, which makes its smoothing window width can adjust depending on CNR. BDS Klobuchar model is utilized to correct the ionospheric model in this paper, and the actual BDS B1 signal is collected for the experimental verification.

The experimental outcomes show that, as for range domain, the overall performance of the adaptive Hatch filter is better than that of the traditional Hatch filter by 28% in the BDS single-frequency receiver without any auxiliary system. At the same time, in the position domain, the RMSE of the suggested algorithm in the horizontal direction and the vertical direction are reduced by 28% and 17%, respectively. Moreover, the proposed algorithm is based on the traditional Hatch

filter structure, which preserves the advantages of simple and easy implementation of the single-frequency positioning. Considering that the development of the BDS single-frequency receiver, such an algorithm is of great value both on theory and practice. Typically, the traditional Hatch filter is applicable for the static GNSS receivers, and the proposed algorithm has prominent performance, especially in the horizontal direction. Whereas its positioning accuracy of the kinematic environments may need further validation.

Acknowledgement

This work is partially supported by the Chinese National Science Foundation (No. 61501079), Doctoral Scientific Research Starting Foundation of Liaoning Province (No. 20170520184 and No. 20170520090), Remote Sensing Youth Science and Technology Innovative Research, Dalian Technology Star Program (No.2017Q058) and the Fundamental Research Funds for the Central Universities (No. 3132018182).

R E F E R E N C E S

[1]. *S.Jin, E.Cardellach and F.Xie*, GNSS Remote Sensing, Springer, Dordrecht, 2014
[2]. *P.Misra and P.Enge*, Global Positioning System: Signals, Measurements, and Performance, Ganga-Jamuna Press: Lincoln, MA, USA, 2010
[3]. *D.K.Elliott and J.H.Christopher*, Understanding GPS: Principles and Applications, Artech House, 2006
[4]. *R.Hatch, R.Sharp and Y.YANG*," An Innovative Algorithm for Carrier-Phase Navigation", in Proc. of the 17th International Technical Meeting of the Satellite Division of the Institute of Navigation, 2004, pp. 1431-1437
[5]. *H.K.Lee, C.Rizos*," Position-domain Hatch filter for kinematic differential GPS/GNSS", in IEEE Transactions on Aerospace and Electronic Systems, **vol. 44**, no. 1, 2008, pp. 30-40
[6]. *X.Zhang and P.Huang*," Optimal Hatch Filter with an adaptive smoothing time based on SBAS", in Proc. of the 2nd International Conference on Soft Computing in Information Communication Technology, 2014, pp. 34–38
[7]. *G.Liu, J.Guo and H.Luo*," Optimal Smoothing of GNSS Pseudo-range by Carrier Phase", in Journal of Spacecraft TT&C Technology, **vol. 34**, no. 2, 2015, pp. 161-167
[8]. *K.Mazher, M.Tahir and K.Ali*," GNSS Pseudorange Smoothing: Linear vs Non-linear Filtering Paradigm", in 2016 IEEE Aerospace Conference, 2016, pp. 1-10
[9]. *B.Park, K.Sohn and C.Kee*," Optimal Hatch Filter with an Adaptive Smoothing Window Width", in Journal of Navigation, **vol. 61**, no. 3, 2008, pp. 435-454
[10]. *Z.Zhou and B.Li*," Optimal Doppler-aided smoothing strategy for GNSS navigation", in GPS Solutions, **vol. 21**, no. 1 , 2017, pp. 197-210
[11]. *J.Jang, H.So, K.Lee and J.Park*," A Theoretical and Experimental Comparison of the Ionosphere-free L1 Pseudorange and the Ionosphere-free Linear Combination Pseudorange by Dual-frequency SBAS Users", in IET Radar, Sonar & Navigation, **vol. 11**, no. 4, 2017, pp. 675-681
[12]. *L.Zhao, L.Li, M.Sun and X.Wang*," Novel Adaptive Hatch Filter to Mitigate the Effects of Ionosphere and Multipath on LAAS", in Journal of Systems Engineering and Electronics, **vol. 21**, no. 6, 2010, pp. 1046–1053

[13]. *G.Chang, T.Xu, C.Chen, B.Ji and S.Li*," Switching Position and Range-domain Carrier Smoothing-code Filtering for GNSS Positioning in Harsh Environments with Intermittent Satellite Deficiencies", in Journal of the Franklin Institute, **vol. 356**, no. 9, 2019, pp. 4928-4947

[14]. *J.Geng, E.Jiang, G.Li, S.Xin and N.Wei*," An Improved Hatch Filter Algorithm towards Sub-Meter Positioning Using only Android Raw GNSS Measurements without External Augmentation Corrections", in Remote Sensing, **vol. 11**, no. 14, 2019

[15]. *Q.Zhang, Z.Chen, F.Rong and Y.Cui*," An Improved Hatch Filter and its Application in Kinematic Positioning with Single-frequency GPS", in Measurement, **vol. 146**, 2019, pp. 868-878

[16]. *O.J.Olwendol, Y.Yamazaki, P.J.Cilliers, P.Baki and P.Doherty*," A Study on the Variability of Ionospheric Total Electron Content over the East African Low-latitude Region and Storm Time Ionospheric Variations", in Radio Science, **vol. 51**, no. 9, 2016, pp. 1503-1518

[17]. *A.Fathy, E.Ghamry and K.Arora*," Mid and low-latitudinal ionospheric field-aligned currents derived from the Swarm satellite constellation and their variations with local time, longitude, and season", in Advances in Space Research, **vol. 64**, no. 8, 2019, pp. 1600-1614

[18]. *M.M.Hoque, N.Jakowski and J.Berdermann*," Ionospheric Correction using NTCM Driven by GPS Klobuchar Coefficients for GNSS Applications", in GPS Solutions, **vol. 21**, no. 4, 2017, pp. 1563-1572

[19]. *W.Roman and S.Damian*," Cardano's Formula, Square Roots, Chebyshev Polynomials and Radicals", in Journal of Mathematical Analysis and Applications, **vol. 362**, no. 2, 2009, pp. 639-647

[20]. *V.T.Tran, N.C.Shivaramaiah and T.D.Nguyen*," Generalised Theory on the Effects of Sampling Frequency on GNSS Code Tracking", in The Journal of Navigation, **vol. 71**, no. 2, 2018, pp. 257-280

[21]. *P.Byungwoon, L.Cheolsoon and Y.Youngsun*," Optimal Divergence-Free Hatch Filter for GNSS Single-Frequency Measurement", in Sensors, **vol. 17**, no. 3, 2017, pp. 448-467